Measurement of Diffused Radon from Earth Crust Locality and Flow Its Path in Air

H. A. S. Aly

Physics Department, Faculty of Girls for Arts, Science and Education, Egypt
Hanan_ali2@women.asu.edu.eg

Abstract: Manually prepared plastic chamber has been designed to detect radon in the chosen field location characterized by presence of uranium ore. Multi detectors were distributed in the all parts of the detector to check the radon path way in the air. Detector A was the detector which faces the coming radon from the underground and record high activity 25775.59 Bq/m^3. Others detectors were recording approximately equal values of radon activity. Ranges of track diameters and depths have been measured, which reflect the incident alpha energy. Finally radon was propagating in all parts of the chamber.

1. Introduction:

Radon diffusion within uranium-bearing wastes has not been taken into account in any safety assessment. This has led to unrealistically high predictions of radiation exposure by radon accompanying shallow land site disposal of uranium-bearing wastes [Tomozo *et al.*, 2008]

One of the most significant (and controversial) sources of radon from uranium mining and milling, both during operation and after rehabilitation, is that from mill tailings. The predictions for radon exhalation and releases have varied significantly, depending on the chosen tailings management regime, although estimates for the same regime can also differ [Gavin, 2007].

Radon exhalation rate affected by the coating layer between uranium ore and detector, this layer attenuate the diffused radon [Kaixuan *et al.*, 2012].

Secular equilibrium is a steady-state condition of equal activities between a long-lived parent radionuclide and its short-lived daughter. The important criteria upon which secular equilibrium depends are [Michael, 2003], i.e. measurements of radon describe indirectly the presence of uranium ore in the tested location, where ^{222}Rn is a decay product of ^{226}Ra which in turn is a decay product of ^{238}U.

The present work has been intended to deduce the path way of radon (^{222}Rn) in air after its decay from subsurface radioactive ore in the earth's crust, to estimate its propagation method in air. Radon chamber has been designed and prepared manually, to flow the radon path and determine its concentration occurred near the Earth's crust.

2. Geological situation of the radioactive ore:

A subsurface radioactive horizon consisted of dolomite siltstone and black shale of 6m thickness is the main target of the study. This anomalously radioactive horizon is incorporated between two sandstone units. The lower sandstone unit is about 30m thickness while the thickness upper one is 20m.Uranium is the main radioactive element in the anomalous horizon, while the thorium is very low in concentrations. Radium has nearly the same activity as uranium, while 40K is vary in concentration. The upper sandstone unit represents the surface at which the detector chamber is fixed well sealed as Fig.2.

3. Methodology:
3.1. CR-39 Set Up in the Radon Chamber:

The irradiation was performed in non ventilated plastic chamber designed and prepared manually in the laboratory. The chamber has a cylindrical shape with height H equal to 21 cm, the diameter of its base is 12 cm and an extended tube T along the chamber axis to penetrate the ground was performed as shown in Fig. 1.

Multi CR-39 detectors, each of area 1cm x 1cm, were distributed inside the chamber to recording alpha particles tracks produced due to decaying of radon and its progenies where, A is a CR-39 detector put on the bottom of the chamber cover face to the window of Tube T, this detector will record alpha particles tracks corresponding to the whole flux of diffused radon emerging from the earth's crust that passing through T, then detectors R_1, R_2, R_3 and R_4 were put on the right side of the chamber such that the distance between them and T level are 4, 8, 12 and 16 cm respectively. Similarly with the same setting detectors L_1, L_2, L_3 and L_4 are put on the left side of the chamber, the intervals were chosen to be nearly equal to the range of alpha particles in air. Finally other CR-39 detectors have been arranged and distributed such that one detector for each quarter of the chamber base namely B_1, B_2, B_3 and B_4.

After arrangements of the detectors over the volume of the chamber as explained above the chamber has been sealed by silicon paste. The chamber has installed in the ground of the studied locality as shown in Fig.2.
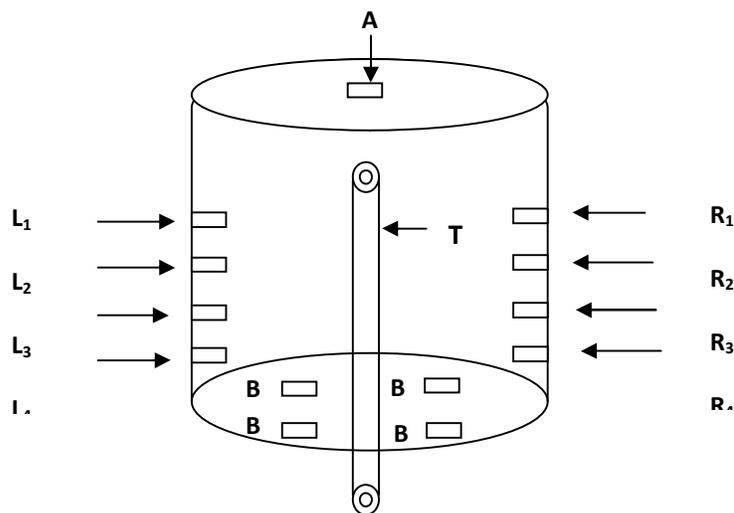

Fig.1 CR-39 Set Up in Radon chamber.

Fig.2 Radon chamber set up in the field.

3.2. Alpha counting:

After three weeks (five radon half lives) of irradiation in the field, for the irradiated and virgin CR39 detectors, were collected and immediately etched chemically in 6.25 N, Na OH, 6 h and constant temperature 70°C with an accuracy of $\pm$ 0.1^{o}C [**AHN** *et al.,* **2005**]. During the etching process the solution was constantly stirred. The detectors were then washed under running distilled water and dried in air.

The detectors were then taken out from the etchant, rinsed with distilled water and dried in air. A piece of etched detector (with the alpha tracks) was then placed inside the mold on the bottom, with the side containing the tracks facing upwards. The track density is counted manually for a number of 100 fields of view. The number of tracks per cm^{2} is then

calculated using a calibration factor which converts the number of tracks observed directly per unit area.

The area of one field of view was calculated by a stage eyepiece and the track density was calculated in terms of tracks per cm^{-2}, the background track density was determined by processing a virgin detector under the same etching conditions, then background was subtracted from the measured track density, in order to obtain realistic statistics of the tracks. The calibration factor of 0.18 ± 0.002 tracks cm^{-2}, obtained from an earlier calibration experiment for the (CR-39) track detector [Khan *et al.,* 1990].

4. Results and Discussion:

Recorded alpha tracks around the whole volume of the chamber, for different distributed detectors in the chamber, have been counted and investigated.

Radon concentrations, tracks diameters range as well as tracks depths range were measured and displayed in the this section.

The concentrations were determined according to the equation given by **Tanner, 1980:**

$$C_{Rn} = \frac{(N - B)}{t C_F} \qquad (3)$$

Where, C_{Rn} is the mean Rn-222 concentration (in Bqm^{-3}), N is the track density (Track.cm^{-2}), B is the background track density (Track.cm^{-2}), C_F is the calibration factor in terms of α- tracks. (cm^{-2} d^{-1}per Bqm^{-3}) and t is the exposure time (hours). Radon concentrations for different detectors positions are listed in Table.1

Tracks for different scanned fields have been outlined by measuring their diameters and depths, range of tracks diameters and depths are listed in Table 1.

Distributions of the radon concentrations inside the chamber are shown in Fig.3, radon concentration recorded by detector A represents the whole radon concentrations diffused from tube T. track diameter is decreased as incident alpha energy was increased while the its depth increased [Khayrat *et al.,*1999]**,** Recorded tracks diameters ranges shown that the

alpha particles reached to the detectors by significant small residual energy relative to the different chamber sites, this situation has been confirmed by the recorded values of tracks depths, where measured tracks diameters and depths for the other chamber sites shown that maximum alpha energy were existed in the chamber base. This explains the slowing down process occurred for radon gas due to multi collisions between its molecules.

Radon distributions for different chamber parts, each separately, are displayed in Figs.4, 5 and 6 for chamber right site, left site and its base respectively.

Exponentially decreasing of radon concentrations have been observed for right and left sites. Right site recorded concentrations value were higher than the left site, this may explains the directions of radon rush, which in turn explains the direction of uranium ore position that is responsible for the generation of measured radon, at the same time this reflect the presence of rock fractures in the left side of the studied locality. A result of the radon concentration on the chamber base has been confirmed the above results where the base right side of the chamber base was characterized by higher concentration than the left side.

Radon concentration recorded by detector A represents the total activity of the emerged radon and entered the chamber through tube T, on the other hand the detectors distributed in the rest chamber will represents the radon activity as well as its progenies.

Other studies for different regions detected highly radon concentrations near uranium ores [Klein *et al.,* 1995, Sadaaki *et al.,* 2002 and Schmidt, 2005 and Sahoo, 2010].

Also radon is strongly related to the porosity of the propagation medium [Mujahid, 2005], the obtained results of radon concentrations not represent the total product radon underground to the studied area where radon diffusion depends strongly on fractures of the hosted rock.

Table.1. Track density, Radon concentrations, Diameters and Depths ranges for different chamber sites.

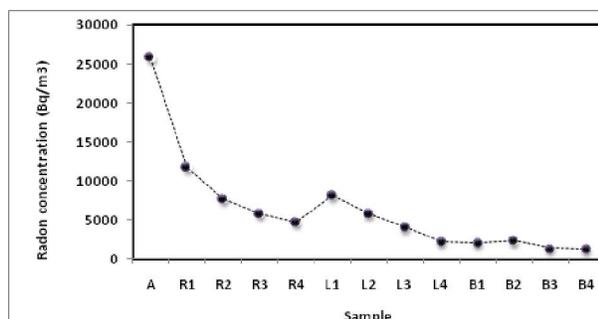| Detector	Track Density (tracks/cm^2)	C (Radon Concentration)	Track Diameter Range (m)	Track Depth Range (m)
A	**97431.72**	**25775.59**	**16.36 – 22.41**	**9.25 – 12.14**
R$_1$	**44231.55**	**11701.47**	**8.44 – 12.37**	**16.44 - 27.3**
R$_2$	**28944.15**	**7657.18**	**5.33 – 9.14**	**24.72 - 31.42**
R$_3$	**21810.03**	**5769.85**	**6.22 – 10.08**	**21.48 – 29.19**
R$_4$	**17733.39**	**4691.37**	**5.88 -11.12**	**19.83 – 30.27**
L$_1$	**30574.81**	**8088.57**	**7.16 – 11.92**	**18.24 –28.14**
L$_2$	**21810.03**	**5769.85**	**6.27 – 8.22**	**27.09 – 29.18**
L$_3$	**15083.57**	**3990.36**	**5.82 – 9.42**	**25.22 – 31.06**
L$_4$	**8132.90**	**2151.56**	**7.56 – 10.33**	**20.91 – 28.56**
B$_1$	**7541.79**	**1995.18**	**5.33 – 6.49**	**29.37 – 31.14**
B$_2$	**8560.95**	**2264.80**	**6.09 – 8.14**	**27.52 – 30.04**
B$_3$	**4891.97**	**1294.17**	**5.19 – 7.08**	**28.81 – 31.61**
B$_4$	**4484.30**	**1186.32**	**4.88 – 7.18**	**27.95 – 33.37**

Fig 3. Radon concentration (Bq/m³) distribution for different chamber parts.
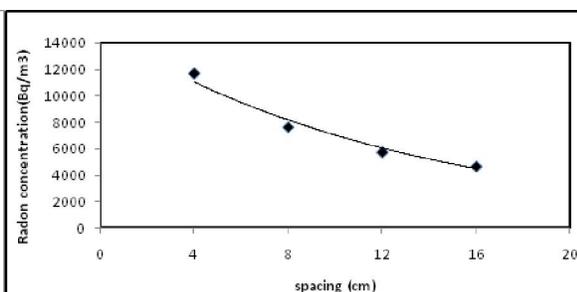

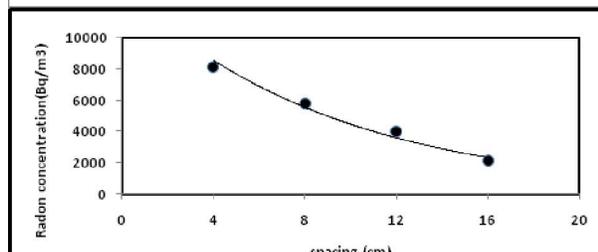**Fig.4.** Radon concentration for different spacing on the chamber right side

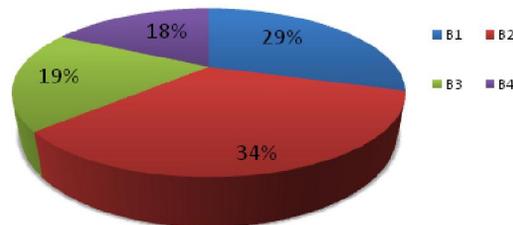**Fig 5.** Radon concentration for different spacing on the chamber left side

Fig.6 Pie shape of radon concentration distributed on the chamber base.

5. Conclusions:

The present work was aimed to flow the pathway of the radon in air. Observed results shown that radon propagate in all direction after it had escape from the earth's crust through the rock fractures. Significant higher radon activity has been recorded and was comparable the uranium ore present in the studied region. The recorded track may be shared between the radon and its progenies.

Acknowledgement:

References:

1. **Gil. Hoon AHN and JAI-KI Lee (2005):** Construction of an environmental radon monitoring system using CR-39 nuclear track detectors, Technical Note , NUCLEAR ENGINEERING AND TECHNOLOGY, vol.37 No.4, 395-400.
2. **Kaixuan Tan, Zehua Liu, Liangshu Xia, JunwenLv, Hanqiao Hu (2012):** The influence of fractal size distribution of covers on radon exhalation from uranium mill tailings.
3. **Khan A.J., A.K. Varshney, R. Parsed, RK. Tyagi and TV.Ramachandran (1990):** Calibration of (CR-39) plastic track detector for the measurement of radon and its daughters in dwellings. Nucl Tracks.RadiatMeasur. vol 17, 497–502.
4. **Khayrat A. H. and S. A. Durrani, (1999):** Variation of alpha-particle track diameter in CR-39 as a function of residual energy and etching conditions, Radiation Measurementsvol 30, Issue 1, 15-18.
5. **Klein D., E. Verchinine, A. Chambaudet, S. Sergeyev And S. Malakhov(1995):** Methodology to Evaluate the Radon Risk Potential: Application in the Kouzbass Region, Radiation Measurements, Vol. 25, Nm 1--4, pp. 635-636.
6. **MICHAEL'ANNUNZIATA F. L. (2003):** Handbook of Radioactivity Analysis, Second Edition, Elsevier Science (USA).
7. **Mudd Gavin M. (2008):** Radon releases from Australian uranium mining and milling projects: assessing the UNSCEAR approach, Journal of Environmental Radioactivity 99 288- 315.
8. **Mujahid S.A., S. Hussain, A.H. Dogar, S. Karim (2005):** Determination of porosity of different materials by radon diffusion, Radiation Measurements 40, 106 – 109.
9. **SadaakiFuruta, Kimio Ito, YuuIshimori (2002):** Measurements of radon around closed uranium mines, Journal of Environmental Radioactivity 62, 97–114
10. **Sahoo B.K., Y.S. Mayya, B.K. Sapra, J.J. Gaware, K.S. Banerjee , H.S. Kushwahaa (2010):** Radon exhalation studies in an Indian uranium tailings pile.
11. **Schmidt P., J. Regner (2005):** Improvement of the radon situation at former uranium mining and milling sites in East Germany, International Congress Series 1276, 238– 239.
12. **Tanner A.B., (1980):** Radon migration in the ground: A supplementary review. Proceedings of Natural Radiation Environment III: Springfield, US DOE Report CONF-780422, vol. 1, 5 – 56.
13. **Tomozo SASAKI1, Yasuyoshi GUNJI and Takao IIDA (2008):** Theoretical Basis for Measuring Small Radon Diffusion Coefficients for a Radium-Bearing Porous Material Generated by Precipitation of Iron (III) Hydroxide, Journal of NUCLEAR SCIENCE and TECHNOLOGY, Vol. 45, No. 7, p. 647–652.

5/13/2013